


# Single-Shot Compressed Photoacoustic Tomographic Imaging with a Single Detector in a Scattering Medium

Yuning Guo<sup>1,\*</sup>, Baowen Li<sup>1,2,†</sup> and Xiaobo Yin<sup>1,2,3,‡</sup>

<sup>1</sup>*Department of Mechanical Engineering, University of Colorado Boulder, Boulder, Colorado 80309, USA*

<sup>2</sup>*Department of Physics, University of Colorado Boulder, Boulder, Colorado 80309, USA*

<sup>3</sup>*Materials Science and Engineering Program, University of Colorado Boulder, Boulder, Colorado 80309, USA*

 (Received 2 August 2019; revised manuscript received 4 February 2020; accepted 17 March 2020; published 3 April 2020)

Photon scattering imposes a fundamental restriction on optical imaging in turbid media. In this work, we propose a compressive-sensing-based photoacoustic imaging modality that allows single-shot tomography with a single detector in a scattering medium. The nonuniform optical speckle grains created in the diffusive regime, which act as a conventional drawback of optical modality, are used to generate ultrasound locally. The photoacoustic signals from spatial positions can be well extracted from a superimposed signal via introduction of locally modulated time delays. Taking advantage of the compressed measurement assisted by the acoustic mask, we demonstrate a theoretical compressed framework of three-dimensional photoacoustic surface tomography with a broad field of view after one-time optical illumination. This approach can increase the photoacoustic imaging efficiency greatly and reveals the potential for dynamic imaging in optically diffusive media.

DOI: [10.1103/PhysRevApplied.13.044009](https://doi.org/10.1103/PhysRevApplied.13.044009)

## I. INTRODUCTION

An outstanding challenge that has continuously attracted the attention of researchers in remote sensing and early diagnosis of diseases is to clearly see objects hidden in turbid media [1,2]. The inherent inhomogeneity of complex conditions, such as smoke, fog, and biological tissue, diffuses optical beams into speckle patterns, limiting the resolution and penetration depth of optical imaging techniques. Recent studies have demonstrated that high-resolution imaging in stable turbid materials could be achieved by many techniques, including multiphoton microscopy [3,4], speckle correlations [5], time reversal [6], guidestar-assisted wave-front shaping [7,8], and transmission matrix techniques [9,10]. Each technique has its advantages and disadvantages; for example, multiphoton microscopy provides optical resolution but generally relies on fluorescence, and memory-effect-based optical techniques deal only with the scattering from a thin enclosing layer. Photoacoustic imaging (PAI), which generates acoustic waves from localized optical absorption via thermal expansion, enables high optical absorption contrast identifiable in an acoustic way [11,12]. By reading the time-of-flight information for a photoacoustic signal, PAI possesses depth-resolved capability and therefore allows three-dimensional

(3D) imaging based on a two-dimensional operation in the scattering medium. Benefiting from wave-front shaping, super-resolution PAI can be realized via a small tagged volume assisted by a guidestar in a scattering environment [13,14]. However, it has a long acquisition time owing to iterative optimizations or a large number of measurements of raster scanning. Thus, a highly efficient PAI approach is desired for application compatible with dynamic scattering environments.

Natural images, which are usually represented sparsely in either the Hadamard domain or the Fourier domain via wavelet transform, a gradient operator, etc., allow one to reconstruct sharp images with undersampled data [15]. Compressive sensing (CS), which can realize image sampling and compression simultaneously on the basis of a randomized sensing mechanism, is able to accelerate data acquisition without significant loss of image quality [15,16]. CS has been successfully applied to hyperspectral imaging, terahertz imaging, magnetic resonance imaging, optical imaging, ultrasound imaging, etc. [1,17–21]. A single-pixel camera, a remarkable implementation of CS, uses a series of random optical patterns for compressed sampling instead of sequential point-by-point sampling [22,23]. Single-pixel imaging with a bucket detector provides a weighted sum of fluctuations arising from all pixels of the object, which could offer enhanced performance, such as higher detection efficiency, faster timing response, and lower dark counts [22]. These enhancements are significant in scenarios where detected intensities are very

\*yuning.guo@colorado.edu

†baowen.li@colorado.edu

‡xiaobo.yin@colorado.edu

weak due to scattering or absorption losses. Thereby, the principle of single-pixel detection is suitable for PAI in the case of biomedical imaging or long-range 3D imaging.

In this work, armed with the principle of single-pixel imaging, we establish single-shot compressed photoacoustic imaging with a single detector that realizes photoacoustic tomographic imaging with just one-time illumination in a scattering medium. With the assistance of spatial sampling based on the speckle distribution, compressed measurement of photoacoustic signals is performed by introducing a spatiotemporally varying ultrasonic field created by an acoustic mask. The proof-of-principle demonstration reveals morphological features of a 3D object with a single measurement in the scattering medium that sheds the light on dynamic imaging in the diffusive regime.

## II. METHOD

Before discussing the compressed photoacoustic imaging, we illuminate some related concepts. Light can go through a scattering medium within the transport mean free path as a diffuse halo, yet the spatial information is scrambled. Formed by partial interference of scrambled wave fronts, the speckle pattern demonstrates a granular structure of diffused intensity distribution as Fig. 1(a) shows. Its statistical properties depend on the properties of the excitation source and the scattering medium (e.g., optical wavelength, anisotropy parameter and scattering length of the medium), which can be estimated by spatial autocorrelation or speckle correlation analysis [24,25]. Besides, a speckle pattern can be generated by the Fourier transform of a random phase matrix in a theoretical simulation.

Figure 1(b) demonstrates the principle of compressed ultrasonic detection with a single detector. A bucket detector collects a superimposed signal  $S(t)$  derived from multiple spatial positions  $P_i(x, y, z)$  on the surface of a 3D object via a temporal measurement. Because of the lack of spatiotemporal diversity, the spatial information for each position cannot be extracted effectively since there are multiple possible decomposition forms of a superimposed signal. An unfocused ultrasound field of randomized frequency sources, together with the localized contribution of the scattering, allows two-dimensional detection by a received channel, which indicates the feasibility of locally monitoring ultrasonic signals [26]. Thereby, a coding mask that introduces a spatiotemporally varying wave field is used to modulate the signal locally [27]. The variations of the mask thickness cause local delays of wave propagation, which results in complex spatiotemporal interference patterns with distorted wave fronts as well as stretched propagation times. Each position in 3D space generates a unique ultrasonic waveform, so the superimposed signal is decomposed exclusively and 3D spatial information regarding the origins can be extracted uniquely. Thereby, 3D ultrasonic compressed sensing is realized with a single measurement

operation. Acting as a coded aperture, an acoustic mask that tags the ultrasonic waves  $S_i(t)$  from spatial positions  $P_i(x, y, z)$  with random time delays  $\Delta T_i$  locally is designed. A simple acoustic mask with position-dependent thickness is displayed in the upper-right panel in Fig. 1(b) for example. It is a plastic plate filled with 200 square bulges with unit size  $L = 0.43$  mm; the thickness of the bulge varies from 1 to 5 mm randomly for each position. According to the Poisson-Kirchhoff formula [28], a bucket detector records a superimposed time-varying ultrasonic signal generated from spatial positions as  $S(t) = \sum S_i(t) * \Delta T_i$  (\* denotes the convolution operation). With the position-dependent time delays, the information regarding each position can be extracted from this superimposed signal with a single measurement.

The transient ultrasonic fields are captured to illuminate the role of the spatiotemporally varying wave field introduced by the acoustic mask. An angular-spectrum algorithm is used to describe the propagation of ultrasonic waves [29]. With pulsed ultrasonic excitation, Fig. 1(c) shows an ultrasonic field behind the acoustic mask (at a fixed depth in the  $x$ - $y$  plane) that demonstrates a spatial-position-dependent intensity distribution. Figure 1(d) shows four transient acoustic fields in the  $x$ - $z$  plane (along with the propagation direction) at time  $t = 12.67, 14.65, 15.90,$  and  $16.83$   $\mu\text{s}$ , respectively. It indicates that the intensity distribution of scrambled wave fronts is temporally dependent during the wave propagation. Thus, the function of the spatiotemporally varying field is clearly revealed in the ultrasonic wave field.

The contrast of ultrasound imaging is determined by acoustic impedance (i.e., the product of sound speed and density), whereas optical absorption contrast determines PAI contrast, which promises the potential for high-resolution PAI with maneuverable optical modulation operations. On optical illumination, a photoacoustic signal is generated from a spatial position at which the sound amplitude and phase are dependent on the optical absorption and local fluence. For the photoacoustic effect governed by a wave equation for pressure [24,30], the pressure  $p_0$  of the generated acoustic wave is expressed as

$$p_0 = \Gamma \mu_a(\mathbf{r}) F(\mathbf{r}), \quad (1)$$

where  $\mu_a(\mathbf{r})$  is the absorption coefficient at position  $\mathbf{r}$  and  $F(\mathbf{r})$  is local light fluence at position  $\mathbf{r}$ . The Grüneisen parameter  $\Gamma$  is expressed as

$$\Gamma = \beta v_s^2 / C_p = \beta / (\kappa \rho C_p), \quad (2)$$

where  $\beta$  is the isobaric-volume-expansion coefficient,  $C_p$  is the specific heat,  $v_s$  is the sound speed,  $\kappa$  is the isothermal compressibility, and  $\rho$  is the mass density [31,32]. When the optical irradiation time is short such that heat conduction can be ignored, the light distribution determines the heated-volume size, and thus the photoacoustic

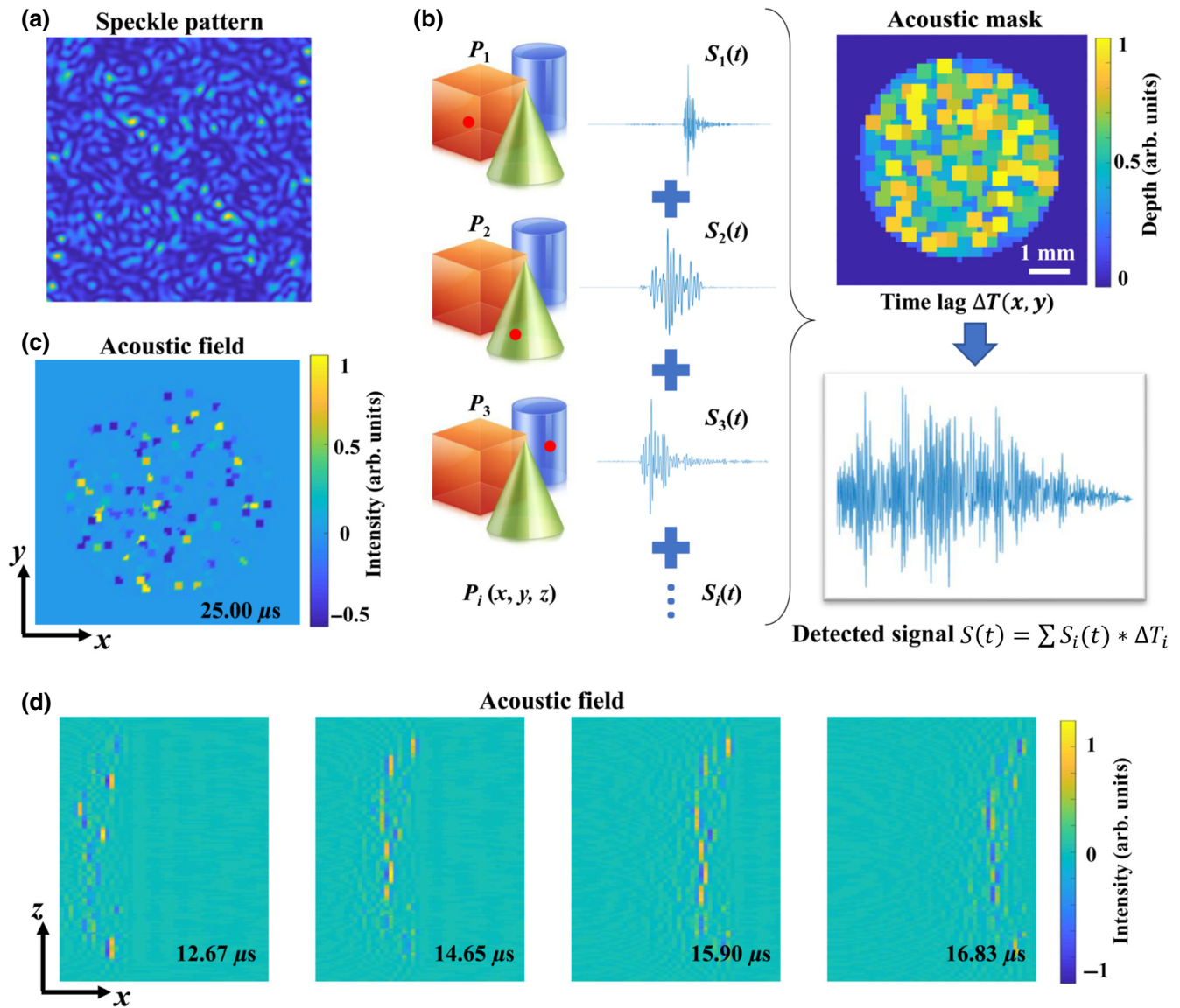


FIG. 1. (a) Speckle pattern. (b) Principle of compressed ultrasonic detection with a single detector. The upper-right panel shows an acoustic mask with position-dependent thickness that provides locally time delays of ultrasonic waves. A bucket detector collects the time-varying ultrasonic signal superimposed from spatial positions as  $S(t) = \sum S_i(t) * \Delta T_i$ . (c) An acoustic field in the  $x$ - $y$  plane captured behind the acoustic mask. (d) Transient acoustic fields in the  $x$ - $z$  plane after the acoustic-mask modulation.

characteristics can be derived from the optical properties [33]. Therefore, a single illumination by multiple optical sources enables multipoint photoacoustic sensing that allows a larger imaging field of view (FOV).

Although the speckled field produced by multiple scattering always plays an undesirable role in optical imaging, the speckle pattern can still be used in some cases; for example, unwrapping hidden information via speckle correlation [34]. In this work, the speckle pattern is exploited as a spatial-position-dependent photoacoustic source. The center frequency of photoacoustic signals varies with the size of the absorber in practical applications [35]. When the speckle size ranges from 10 to 100  $\mu m$ , the center

frequency of generated ultrasonic waves ranges from 10 to 100 MHz in water. Sensing ultrasonic waves excited by a speckle pattern with size approaching the optical diffraction limit could be difficult by a conventional ultrasonic transducer. However, the speckle size could be larger than the scale of the diffraction limit via either enlargement in free-space propagation or within the phase evolution in the diffusive regime inside a volumetric scattering medium. Furthermore, ultrasound detection can achieve acoustic-diffraction-unlimited listening by some approaches; for example, an ultrasonic superoscillation lens and metamaterials via acoustic deep subwavelength focusing, and the nonlinear photoacoustic effect [36–38]. With consideration

of the sensitivity distribution of ultrasonic detection, it is therefore possible to sense the photoacoustic signal generated from a speckle size of tens of micrometers by ultrasonic detection under some circumstances.

### III. MODELING AND RESULTS

Figure 2 schematically illustrates the setup of the single-shot compressed-PAI system. A speckle pattern consisting of a collection of speckle grains provides nonuniform, position-dependent illumination of spatial positions of an object (either in a scattering medium or behind it) to generate multiple photoacoustic signals. As the acoustic mask with spatially varying thickness introduces local time delays, phase uniformity of the backscattered ultrasonic waves is perturbed and therefore random deterministic interference patterns are produced. A single-element ultrasonic transducer finally collects the perturbed ultrasonic waves as a superimposed temporally dependent photoacoustic signal according to the angular-spectrum algorithm. The detection of 3D spatial information for an object is turned into a single temporal measurement with a bucket detector, which indicates compressed sensing of the photoacoustic signal. “Single shot” denotes capturing the entire real-time dynamic process without repeating the event [39]. That is, a single measurement is able to record the actual duration in which an event occurs. Since the measurement of the photoacoustic wave is acquired once by a single detector with one-time illumination, our compressed-PAI system can be treated as single-shot photoacoustic imaging.

The numerical principles involved are introduced in the following. For the proposed compressed-PAI system here, the recorded photoacoustic signal can be regarded as a linear combination of scattered signals transmitted from different spatial positions. The signal  $\mathbf{u}$ , a vector containing the sampled signals, is linearly related to the vector  $\mathbf{v}$  of an image as  $\mathbf{u} = \mathbf{H}\mathbf{v} + \mathbf{n}$ , where  $\mathbf{H}$  is the measurement matrix and the vector  $\mathbf{n}$  denotes the noise.  $\mathbf{u}$  possesses a length of  $K$ , which is the number of temporal samplings. The measurement matrix  $\mathbf{H}$  has a size of  $K \times N$ , where  $N$  is the number of voxels. Determined by the measurement process,  $\mathbf{H}$  represents the spatiotemporal distribution of signals within a 3D volume and is constructed by calibration from the transmission field.

The entire spatiotemporal wave field is required to obtain the elements of  $\mathbf{H}$ . The impulse signals in a plane closely behind the mask surface (perpendicular to the propagation axis) are spatially mapped first. Then the recorded field will propagate to any parallel plane according to the angular-spectrum approach over time. Thus, the spatiotemporal information for each spatial point in 3D space can be computed and the columns of  $\mathbf{H}$  are populated subsequently. Calibration is required for specific acoustic masks and sensors. Considering the temporal bandwidth as well as the mask thickness, it is hard to guarantee the signals modulated by mask pixels are uncorrelated. To add more diversity to the pixels, a speckle pattern that possesses spatially dependent grains with nonuniform sizes serves as an additive spatial sampling of the object. That can increase the uncorrelation of modulated signals and improve the resolvability of perturbed ultrasonic waves. In addition, the influence of the signal scattered by the detector on the

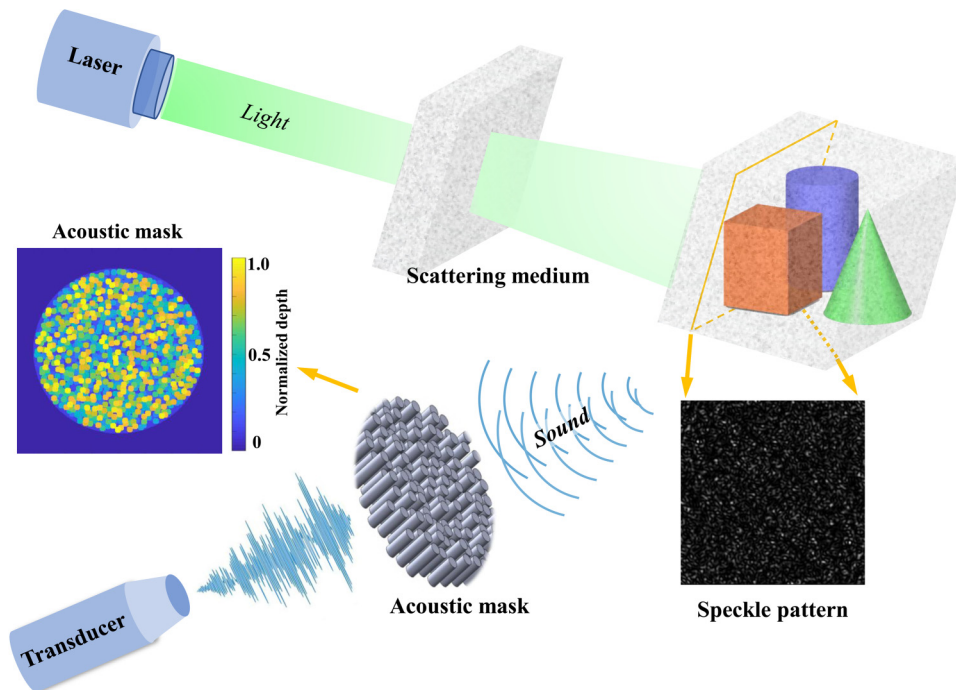


FIG. 2. Single-shot compressed photoacoustic imaging. An object is illuminated by the speckled field formed through or inside a scattering medium. The generated photoacoustic signals from spatial positions of an object are recorded by a single ultrasonic transducer after modulation by an acoustic mask.

recorded signal is considered in the spatiotemporal wave field. On the basis of time reversal [40], the numerical amendment is implemented in the  $\mathbf{H}$  construction by our considering the convolution of the transmitted signal and the scattered signal produced by the sensor. As the sampled signals after the measurement of  $\mathbf{H}$  are typically uncorrelated in our system, the sparse image can be successfully reconstructed with fewer measurements than the number of voxels, even with a single measurement.

After the superimposed signal has been recorded, the last step is to reconstruct the image with appropriate algorithms. Three-dimensional photoacoustic imaging inversion is basically a problem of integral geometry, which can be attributed to the  $\ell_1$ -minimization problem and handled via convex optimization methods [15]. An image  $\mathbf{v}$  can be presented sparsely in a certain domain with an invertible sparse matrix  $\boldsymbol{\psi}$  as the representation  $\mathbf{f} = \boldsymbol{\psi}\mathbf{v}$ . The measurement can be expressed as  $\mathbf{u} = \mathbf{H}\boldsymbol{\psi}^{-1}\mathbf{f}$ . When the transmission matrix  $\mathbf{H}\boldsymbol{\psi}^{-1}$  satisfies the restricted isometry property,  $\ell_1$  regularization is used to estimate  $\mathbf{f}$  from  $\mathbf{u}$  and obtain the image  $\mathbf{v} = \boldsymbol{\psi}^{-1}\mathbf{f}$ . When the image  $\mathbf{v}$  is already sparse, the sparse matrix  $\boldsymbol{\psi}$  is the identity matrix  $\mathbf{I}$  and the measurement is presented as  $\mathbf{u} = \mathbf{H}\mathbf{v}$ . Given a recorded signal  $\mathbf{u}$ , an optimal sparse image  $\mathbf{v}^*$  can be sought by solving a standard basis pursuit problem

$$\mathbf{v}^* = \arg \min_{\mathbf{v}} \|\mathbf{v}\|_{\ell_1} \quad \text{subject to} \quad \mathbf{H}\mathbf{v} = \mathbf{u}, \quad (3)$$

which is processed by the  $\ell_1$ -MAGIC package based on a primal-dual algorithm [41]. A least-squares estimation of  $\mathbf{v}$ , serving as an initial value for the primal-dual algorithm, is obtained with LSQR (an algorithm for sparse linear equations and least-squares problems) [42]

$$\tilde{\mathbf{v}} = \arg \min_{\mathbf{v}} \frac{1}{2} \|\mathbf{H}\mathbf{v} - \mathbf{u}\|_{\ell_2}^2. \quad (4)$$

The numerical algorithms are implemented in MATLAB R2018b.

We now provide a sparse 3D object consisting of two letters as a proof-of-principle demonstration of high-efficiency single-shot compressed PAI. The sparse object and the transducer are set in a simulated water environment and the corresponding Grüneisen parameter is 0.12 at 22 °C [31]. The FOV in the  $x$ - $y$  plane is 5 mm  $\times$  5 mm, which is divided into 100  $\times$  100 pixels. The depth ( $z$  direction) is composed of six selected slices with interval  $\Delta = 150 \mu\text{m}$ . A speckle pattern acquired from the observation plane behind a diffuser, which has a speckle size of 100  $\mu\text{m}$ , is used as the photoacoustic source. As a 10-MHz transducer with a wavelength of 148  $\mu\text{m}$  is used in the simulated water environment, the recorded photoacoustic signal can be delayed by one wavelength with a local thickness of 343  $\mu\text{m}$  (the mask density is 2600 m/s). The acoustic mask here is a plate filled with 400 randomly

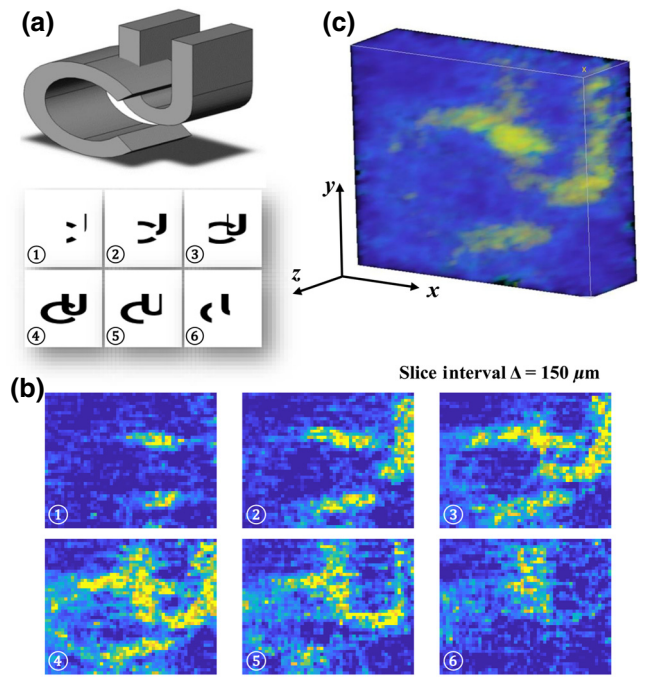


FIG. 3. (a) The prototype of a 3D object and six selected slices with depth interval  $\Delta = 150 \mu\text{m}$ . (b) The recovered slices and (c) the reconstructed 3D image based on single-shot compressed PAI.

distributed cylinders ( $r = 0.15 \text{ mm}$ ), in which the thickness of the cylinders ranges from 0.1 to 1 mm randomly (see the inset in Fig. 2), which allows the acoustic times of flight to be modulated position dependently. The morphological features with a broad FOV can be observed from the 3D reconstructed object and two-dimensional images in Fig. 3. The details of the recovered slices at different depths agree well with the corresponding prototypes, which shows the depth-resolved capability of compressed PAI. This demonstration indicates the compressed capability of single-shot PAI with a single detector; for example, the surface tomographic features of a 3D object can be reconstructed with just one-time illumination together with a single measurement in an optically diffusive medium.

#### IV. CONCLUDING REMARKS

The proposed single-shot compressed photoacoustic tomographic imaging gets rid of sequential measurements, in which the acquisition time mainly relies on the propagation time of ultrasonic waves. The actual duration of the photoacoustic signal from generation to detection is estimated to be on the scale of submilliseconds for a propagation distance of tens of centimeters. When the acquisition time is shorter than a speckle decorrelation time on the order of 1 ms, single-shot compressed imaging

reveals a potential for *in vivo* applications as the scattering property is deterministic. It should be noted that a well-developed speckle pattern in which the size is on the order of optical wavelength would severely hinder effective sensing of diverse photoacoustic signals, which imposes restrictions on *in vivo* applications of the proposed compressed PAI. Although the reconstruction time may exceed the acquisition time for a complex object, it has little influence on information acquisition, which is still promising for real-time recording environments. Several approaches could be used to yield better imaging quality of this single-shot compressed PAI; for example, increasing the pixel number of the acoustic mask, generating optimized structured illumination, and rotating the sample or using multiple detectors to obtain an omnidirectional view of the 3D object. Besides, more-accurate and more-efficient algorithms, (e.g., based on machine learning) will be considered to reconstruct 3D features. Moreover, as PAI can resolve a complex material with various photoabsorbing properties, compressed multispectral imaging is also an exciting direction worthy of pursuit. Revealing the potential of high-speed imaging, the single-shot single-detector approach has made great progress in the photoacoustic field recently [43–45]; for example, realizing wide-field imaging via introduction of an ergodic relay, achieving one waveform reconstruction by acoustic-scattering-mediated encoding. Furthermore, high-resolution functional photoacoustic imaging, which directly visualizes dynamics in biomedical processes, has been conducted on *in vivo* small-animal models at the whole-body scale [46].

In summary, a single-shot photoacoustic imaging system based on compressive sensing is proposed that achieves surface tomographic imaging with a single detector in a scattering medium. An acoustic mask is used to introduce a spatiotemporally varying field on the photoacoustic signals, which allows spatial information originating from spatial positions to be extracted uniquely. The speckle pattern, which evolves from the inherent inhomogeneity of a scattering medium, acts as a randomly-position-dependent photoacoustic source. Taking advantage of compressed sampling implemented by the acoustic mask together with the auxiliary sampling of the speckled field, the compressed PAI is capable of resolving 3D spatial information with a broad FOV via a single measurement operation. Thus, the morphological features of a 3D object can be visualized in a high-efficiency way, which offers promise for real-time tomographic imaging in dynamic environments and biomedical applications.

#### ACKNOWLEDGMENTS

Y.G. appreciates beneficial discussions with Dr. C. Hou. Y.G. is grateful to the Acoustical Society of America for F. V. Hunt Postdoctoral Fellowship, and for

partial support by the seed fund from Interdisciplinary Research Theme—Imaging Science at the College of Engineering and Applied Sciences, University of Colorado Boulder.

- 
- [1] A. P. Mosk, A. Lagendijk, G. Lerosey, and M. Fink, Controlling waves in space and time for imaging and focusing in complex media, *Nat. Photonics* **6**, 283 (2012).
  - [2] J. Bertolotti, E. G. van Putten, C. Blum, A. Lagendijk, W. L. Vos, and A. P. Mosk, Non-invasive imaging through opaque scattering layers, *Nature* **491**, 232 (2012).
  - [3] F. Helmchen and W. Denk, Deep tissue two-photon microscopy, *Nat. Methods* **2**, 932 (2005).
  - [4] A. Escobet-Montalbán, R. Spesyvtsev, M. Chen, W. A. Saber, M. Andrews, C. S. Herrington, M. Mazilu, and K. Dholakia, Wide-field multiphoton imaging through scattering media without correction, *Sci. Adv.* **4**, eaau1338 (2018).
  - [5] O. Katz, P. Heidmann, M. Fink, and S. Gigan, Non-invasive single-shot imaging through scattering layers and around corners via speckle correlations, *Nat. Photonics* **8**, 784 (2014).
  - [6] B. Judkewitz, Y. M. Wang, R. Horstmeyer, A. Mathy, and C. Yang, Speckle-scale focusing in the diffusive regime with time reversal of variance-encoded light (TROVE), *Nat. Photonics* **7**, 300 (2013).
  - [7] R. Horstmeyer, H. Ruan, and C. Yang, Guidestar-assisted wavefront-shaping methods for focusing light into biological tissue, *Nat. Photonics* **9**, 563 (2015).
  - [8] D. B. Conkey, A. M. Caravaca-Aguirre, J. D. Dove, H. Ju, T. W. Murray, and R. Piestun, Super-resolution photoacoustic imaging through a scattering wall, *Nat. Commun.* **6**, 7902 (2015).
  - [9] S. M. Popoff, G. Lerosey, M. Fink, A. C. Boccara, and S. Gigan, Controlling light through optical disordered media: Transmission matrix approach, *New J. Phys.* **13**, 123021 (2011).
  - [10] T. Chaigne, O. Katz, A. C. Boccara, M. Fink, E. Bossy, and S. Gigan, Controlling light in scattering media non-invasively using the photoacoustic transmission matrix, *Nat. Photonics* **8**, 58 (2014).
  - [11] The general optoacoustic conversion mechanisms include deformation potential, thermoelasticity, radiation pressure, inverse piezoelectric process, and electrostriction. In non-piezoelectric materials, only the first-two mechanisms are considered. For general scattering media, such as biological tissue, the motion of electrons contributes little to energy transfer and therefore the mechanism of deformation potential is ignored and only thermoelasticity is studied in this paper.
  - [12] L. V. Wang and J. Yao, A practical guide to photoacoustic tomography in the life sciences, *Nat. Methods* **13**, 627 (2016).
  - [13] S. Rotter and S. Gigan, Light fields in complex media: Mesoscopic scattering meets wave control, *Rev. Mod. Phys.* **89**, 015005 (2017).
  - [14] J.-H. Park, Z. Yu, K. Lee, P. Lai, and Y. Park, Perspective: Wavefront shaping techniques for controlling multiple light

- scattering in biological tissues: Toward *in vivo* applications, *APL Photonics* **3**, 100901 (2018).
- [15] E. J. Candes, J. Romberg, and T. Tao, Robust uncertainty principles: Exact signal reconstruction from highly incomplete frequency information, *IEEE Trans. Inf. Theory* **52**, 489 (2006).
- [16] R. G. Baraniuk, Compressive sensing, *IEEE Signal Process. Mag.* **24**, 118 (2007).
- [17] M. Lustig, D. Donoho, and J. M. Pauly, Sparse MRI: The application of compressed sensing for rapid MR imaging, *Magn. Reson. Med.* **58**, 1182 (2007).
- [18] M. Süzen, A. Giannoula, and T. Durduran, Compressed sensing in diffuse optical tomography, *Opt. Express* **18**, 23676 (2010).
- [19] C. Quinsac, A. Basarab, J. Girault, and D. Kouamé, in *2010 IEEE Workshop On Signal Processing Systems*, (2010), p. 231–236.
- [20] A. Liutkus, D. Martina, S. Popoff, G. Chardon, O. Katz, G. Lerosey, S. Gigan, L. Daudet, and I. Carron, Imaging with nature: Compressive imaging using a multiply scattering medium, *Sci. Rep.* **4**, 5552 (2014).
- [21] C. M. Watts, D. Shrekenhamer, J. Montoya, G. Lipworth, J. Hunt, T. Sleasman, S. Krishna, D. R. Smith, and W. J. Padilla, Terahertz compressive imaging with metamaterial spatial light modulators, *Nat. Photonics* **8**, 605 (2014).
- [22] M. P. Edgar, G. M. Gibson, and M. J. Padgett, Principles and prospects for single-pixel imaging, *Nat. Photonics* **13**, 13 (2018).
- [23] M. F. Duarte, M. A. Davenport, D. Takhar, J. N. Laska, T. Sun, K. F. Kelly, and R. G. Baraniuk, Single-pixel imaging via compressive sampling, *IEEE Signal Process. Mag.* **25**, 83 (2008).
- [24] E. Bossy and S. Gigan, Photoacoustics with coherent light, *Photoacoustics* **4**, 22 (2016).
- [25] C. A. Thompson, K. J. Webb, and A. M. Weiner, Imaging in scattering media by use of laser speckle, *J. Opt. Soc. Am. A* **14**, 2269 (1997).
- [26] G. T. Clement, Two-dimensional ultrasound detection with unfocused frequency-randomized signals, *J. Acoust. Soc. Am.* **121**, 636 (2007).
- [27] P. Kruizinga, P. van der Meulen, A. Fedjajevs, F. Mastik, G. Springeling, N. de Jong, J. G. Bosch, and G. Leus, Compressive 3D ultrasound imaging using a single sensor, *Sci. Adv.* **3**, e1701423 (2017).
- [28] M. Born and E. Wolf, *Principles of Optics: Electromagnetic Theory of Propagation, Interference and Diffraction of Light* (Elsevier, 2013).
- [29] Y. Du, H. Jensen, and J. A. Jensen, Investigation of an angular spectrum approach for pulsed ultrasound fields, *Ultrasonics* **53**, 1185 (2013).
- [30] G. J. Diebold, T. Sun, and M. I. Khan, Photoacoustic Monopole Radiation in one, two, and Three Dimensions, *Phys. Rev. Lett.* **67**, 3384 (1991).
- [31] D.-K. Yao, C. Zhang, K. I. Maslov, and L. V. Wang, Photoacoustic measurement of the grüneisen parameter of tissue, *J. Biomed. Opt.* **19**, 017007 (2014).
- [32] L. V. Wang and L. Gao, Photoacoustic microscopy and computed tomography: From bench to bedside, *Annu. Rev. Biomed. Eng.* **16**, 155 (2014).
- [33] G. Paltauf, H. Schmidt-Kloiber, and H. Guss, Light distribution measurements in absorbing materials by optical detection of laser-induced stress waves, *Appl. Phys. Lett.* **69**, 1526 (1996).
- [34] H. Yu, K. Lee, J. Park, and Y. Park, Ultrahigh-definition dynamic 3D holographic display by active control of volume speckle fields, *Nat. Photonics* **11**, 186 (2017).
- [35] J. Sun, B. Zhang, Q. Feng, H. He, Y. Ding, and Q. Liu, Photoacoustic wavefront shaping with high signal to noise ratio for light focusing through scattering media, *Sci. Rep.* **9**, 4328 (2019).
- [36] J. Hyun, Y. T. Kim, I. Doh, B. Ahn, K. Baik, and S.-H. Kim, Realization of an ultrathin acoustic lens for subwavelength focusing in the megasonic range, *Sci. Rep.* **8**, 9131 (2018).
- [37] S. Zhang, L. Yin, and N. Fang, Focusing Ultrasound with an Acoustic Metamaterial Network, *Phys. Rev. Lett.* **102**, 194301 (2009).
- [38] P. Lai, L. Wang, J. W. Tay, and L. V. Wang, Photoacoustically guided wavefront shaping for enhanced optical focusing in scattering media, *Nat. Photonics* **9**, 126 (2015).
- [39] J. Liang and L. V. Wang, Single-shot ultrafast optical imaging, *Optica* **5**, 1113 (2018).
- [40] M. Fink, Time reversal of ultrasonic fields. I. Basic principles, *IEEE Trans. Ultrason. Ferroelectr. Freq. Control* **39**, 555 (1992).
- [41]  $\ell 1$ -magic code and the User's Guide are available from <https://statweb.stanford.edu/~candes/software/l1magic/index.html#code>.
- [42] C. C. Paige and M. A. Saunders, LSQR: An algorithm for sparse linear equations and least squares, *ACM Trans. Math. Software (TOMS)* **8**, 195 (1982).
- [43] Y. Li, L. Li, L. Zhu, K. Maslov, J. Shi, P. Hu, E. Bo, J. Yao, J. Liang, L. Wang, and L. V. Wang, Snapshot photoacoustic topography through an ergodic relay for high-throughput imaging of optical absorption, *Nat. Photonics* **14**, 164 (2020).
- [44] X. L. Deán-Ben, A. Özbek, H. López-Schier, and D. Razansky, Acoustic Scattering Mediated Single Detector Photoacoustic Tomography, *Phys. Rev. Lett.* **123**, 174301 (2019).
- [45] N. Huynh, F. Lucka, E. Z. Zhang, M. M. Betcke, S. R. Arridge, P. C. Beard, and B. T. Cox, Single-pixel camera photoacoustic tomography, *J. Biomed. Opt.* **24**, 121907 (2019).
- [46] L. Li, L. Zhu, C. Ma, L. Lin, J. Yao, L. Wang, K. Maslov, R. Zhang, W. Chen, J. Shi, and L. V. Wang, Single-impulse panoramic photoacoustic computed tomography of small-animal whole-body dynamics at high spatiotemporal resolution, *Nat. Biomed. Eng.* **1**, 0071 (2017).